Human Molecular Genetics, 2017, Vol. 26, No. 22 4406–4415

doi: 10.1093/hmg/ddx326
Advance Access Publication Date: 22 August 2017
Original Article

ORIGINAL ARTICLE

A pathogenic S250F missense mutation results in a mouse model of mild aromatic L-amino acid decarboxylase (AADC) deficiency

Charlotte Caine[1,2,†], Meytal Shohat[1,2,†], Jeong-Ki Kim[1,2], Koki Nakanishi[3], Shunichi Homma[3], Eugene V. Mosharov[4,5,6] and Umrao R. Monani[1,2,4,*]

[1]Department of Pathology and Cell Biology, [2]Center for Motor Neuron Biology and Disease, [3]Department of Medicine, [4]Department of Neurology, [5]Department of Psychiatry, Columbia University Medical Center, New York, NY 10032, USA and [6]New York State Psychiatric Institute, New York, NY 10032, USA

*To whom correspondence should be addressed at: Department of Pathology & Cell Biology, Columbia University, P&S, Room 5-422, 630 W. 168th St., New York, NY 10032, USA. Tel: +1 2123425132; Fax: +1 2123055438; Email: um2105@columbia.edu

Abstract

Homozygous mutations in the aromatic L-amino acid decarboxylase (AADC) gene result in a severe depletion of its namesake protein, triggering a debilitating and often fatal form of infantile Parkinsonism known as AADC deficiency. AADC deficient patients fail to produce normal levels of the monoamine neurotransmitters dopamine and serotonin, and suffer a multi-systemic disorder characterized by movement abnormalities, developmental delay and autonomic dysfunction; an absolute loss of dopamine is generally considered incompatible with life. There is no optimal treatment for AADC deficiency and few truly good models in which to investigate disease mechanisms or develop and refine therapeutic strategies. In this study, we introduced a relatively frequently reported but mildly pathogenic S250F missense mutation into the murine *Aadc* gene. We show that mutants homozygous for the mutation are viable and express a stable but minimally active form of the AADC protein. Although the low enzymatic activity of the protein resulted in only modestly reduced concentrations of brain dopamine, serotonin levels were markedly diminished, and this perturbed behavior as well as autonomic function in mutant mice. Still, we found no evidence of morphologic abnormalities of the dopaminergic cells in mutant brains. The striatum as well as substantia nigra appeared normal and no loss of dopamine expressing cells in the latter was detected. We conclude that even minute levels of active AADC are sufficient to allow for substantial amounts of dopamine to be produced in model mice harboring the S250F mutation. Such mutants represent a novel, mild model of human AADC deficiency.

Introduction

Aromatic L-amino acid decarboxylase (AADC) is a pyridoxal phosphate-dependent enzyme responsible for catalyzing the final step in the production of the monoamine neurotransmitters, dopamine and serotonin (1,2). Dopamine underlies the control of voluntary movement, the modulation of behavior, reward-based learning and the regulated release of various hormones. It is also a precursor of the catecholamines, noradrenaline and adrenaline. Serotonin serves as the substrate for melatonin, and is an important neuromodulator, regulating gastrointestinal function, the respiratory and cardiovascular systems, circadian rhythm, body temperature and the sensation of pain. Paucity of AADC therefore impacts many of the myriad physiological functions associated with dopamine, serotonin

[†]The authors wish it to be known that, in their opinion, the first two authors should be regarded as joint First Authors.
Received: May 21, 2017. **Revised:** July 23, 2017. **Accepted:** August 15, 2017

and their metabolites, and results in the rare but potentially life-threatening autosomal recessive disorder, AADC deficiency (3–8). AADC deficient patients become symptomatic as infants and characteristically exhibit hypotonia, hypokinesia, choreoathetosis and oculogyric crises. Autonomic dysfunction in these patients encompasses nasal congestion, diaphoresis and temperature instability (8).

AADC deficiency is customarily treated with monoamine oxidase (MAO) inhibitors, vitamin B_6, usually in the form of pyridoxine, dopamine agonists or some combination thereof, but patients generally respond poorly, and those on the more severe end of the disease spectrum often succumb to the disorder during the first decade of life (3,8,9). A gene replacement strategy in four patients reportedly provided therapeutic benefit, but appeared to restore protein to only localized regions of the putamen, failed to greatly alter disease biomarkers and triggered dyskinesias or severe apnea in a proportion of the treated individuals (10). Accordingly, there is still an unmet medical need for a safe, reliable and effective treatment for human AADC deficiency.

AADC deficiency was initially described in 1990 and involved an instance of relatively mildly affected monozygotic twins who were found to harbor a homozygous mutation in the *AADC* gene, have markedly low levels of AADC activity and correspondingly little homovanillic acid (HVA) and 5-hydroxyindoleacetic acid (5-HIAA)—catabolic products respectively of dopamine and serotonin (11). Consistent with the signature features of the disease, cerebrospinal fluid (CSF) levels of 3,4-dihydroxyphenylalanine (L-Dopa) and 5-hydroxytryptophan (5-HTP), precursors, respectively, of dopamine and serotonin, were grossly—12–15 times normal values—elevated and blood serotonin reduced by ∼95% in the patients (11). Following the initial description of the disease, ∼100 additional cases have been reported involving ∼28 different missense mutations (12). Although a definitive genotype–phenotype correlation has not emerged from the literature, patients harboring an intron 6 splice-site mutation, reportedly more frequent in the Chinese population, are more severely affected. In contrast, individuals, including the index cases, bearing a relatively frequent homozygous S250F mutation are milder. In an attempt to model AADC deficiency and better understand the human disease, Lee *et al.* knocked in the IVS 6+4A>T splice site mutation into the mouse genome (13). However, the mutation, devoid of an accompanying neo selection cassette, failed to mimic the splicing error observed in human patients, resulting in mice that were reportedly disease-free. Retention of the neo cassette within the engineered allele disrupted protein expression and triggered disease, but the resulting mutants do not owe their phenotype to a *bona fide* human mutation. In contrast, ablating murine AADC by excising exon 8 fails to produce viable mice, rendering it impossible to study the disease postnatally in constitutive knockouts (14). In this study, we report a novel mouse model of AADC deficiency that harbors the S250F mutation identified in the index patients. We show that although model mice are viable they express profoundly low levels of active AADC. Yet, dopamine levels in the basal ganglia of the mice were only modestly altered and neurons in the substantia nigra remained intact. In contrast, we found that serotonin levels in the mutants were markedly reduced and this perturbed behavior as well as autonomic function. We conclude that even minimal amounts of active AADC are sufficient to produce significant concentrations of dopamine and that low amounts of the enzyme *per se* do not impact the dopaminergic system. The AADC S250F mutant mouse we report here is expected to serve as a useful tool in the pre-clinical development of effective therapies for human AADC deficiency.

Results

Generation of AADC S250F mutant mice

To create our murine model of AADC deficiency, we exploited an 835C>T missense mutation in exon 7 of the human *AADC* gene. The C>T change induces a S250F amino acid alteration in the AADC protein sequence and constitutes both the initial as well as second most commonly reported genetic lesion in AADC deficiency (4,11). Importantly, the serine residue that is replaced at this position by the mutation constitutes part of a highly conserved five amino acid domain, a suggestion that it is of structural and/or functional importance to the AADC protein (Fig. 1A). To mutate the corresponding amino acid in the murine genome to a phenylalanine, a knock-in strategy was employed. This involved a C>T change at position 890 of the murine *Aadc* gene; the targeting strategy is depicted in Figure 1B. Following electroporation of the targeting construct into embryonic stem (ES) cells, correctly targeted clones were identified by PCR and then confirmed by Southern blot analysis (Fig. 1C). They were then introduced into mouse blastocysts to generate knock-in mice. This resulted in the derivation of a single founder whose heterozygous state was detected by PCR and then confirmed by sequence analysis (Fig. 1D). The founder was further documented to transmit the mutant *Aadc* allele through the germline to his progeny.

To generate mice homozygous for the S250F mutation, carrier mice were bred. On a mixed (C57Bl/6; FVB/N) genetic background, we found that homozygous ($Aadc^{S250F/S250F}$) mutants were indeed viable but observed at a significantly lower frequency than expected from a heterozygous cross (8% versus 25%; also see Supplementary Material, Fig. S1). Consistent with this observation, an analysis of E15.5 embryos resulting from timed pregnancies revealed a subset of mutants that appeared shriveled, poorly developed, grossly dysmorphic and most unlikely to progress to term (Supplementary Material, Fig. S1E). In an attempt to increase the numbers of homozygous mutants, we bred $Aadc^{S250F/S250F}$ males with heterozygous ($Aadc^{+/S250F}$) females. While this strategy did hasten the generation of $Aadc^{S250F/S250F}$ mutants, we once again noted a markedly reduced (Observed—14%; Expected—50%) frequency of these animals (Supplementary Material, Fig. S1). Interestingly, breeding $Aadc^{S250F/S250F}$ females with heterozygous or wild-type (WT) males resulted in litters of no more than two to three pups none of which survived beyond 48 h owing to poor maternal care. To determine whether purifying strain background would normalize the frequency of obtaining mutant animals, we backcrossed $Aadc^{+/S250F}$ heterozygotes over five successive generations to each of the C57Bl/6 and FVB/N strains, respectively. Carrier mice were then bred to obtain mutants. Intriguingly, we found that purifying strain background exacerbated the situation, resulting in litters totally devoid of $Aadc^{S250F/S250F}$ mice (Supplementary Material, Fig. S1). We draw several conclusions from these observations. First, while mutants on a mixed background are viable and, indeed, reach maturity, a significant proportion does not survive embryonic development and is likely resorbed during gestation. Second, mixed background male mutants that do survive and reach adulthood are fertile and able to breed. In contrast, female $Aadc^{S250F/S250F}$ mice have a greatly reduced fertility and exhibit poor maternal care, the latter a likely result of lowered serotonin levels which have also been reported by others to underlie this abnormality in behavior (15). Finally, our results

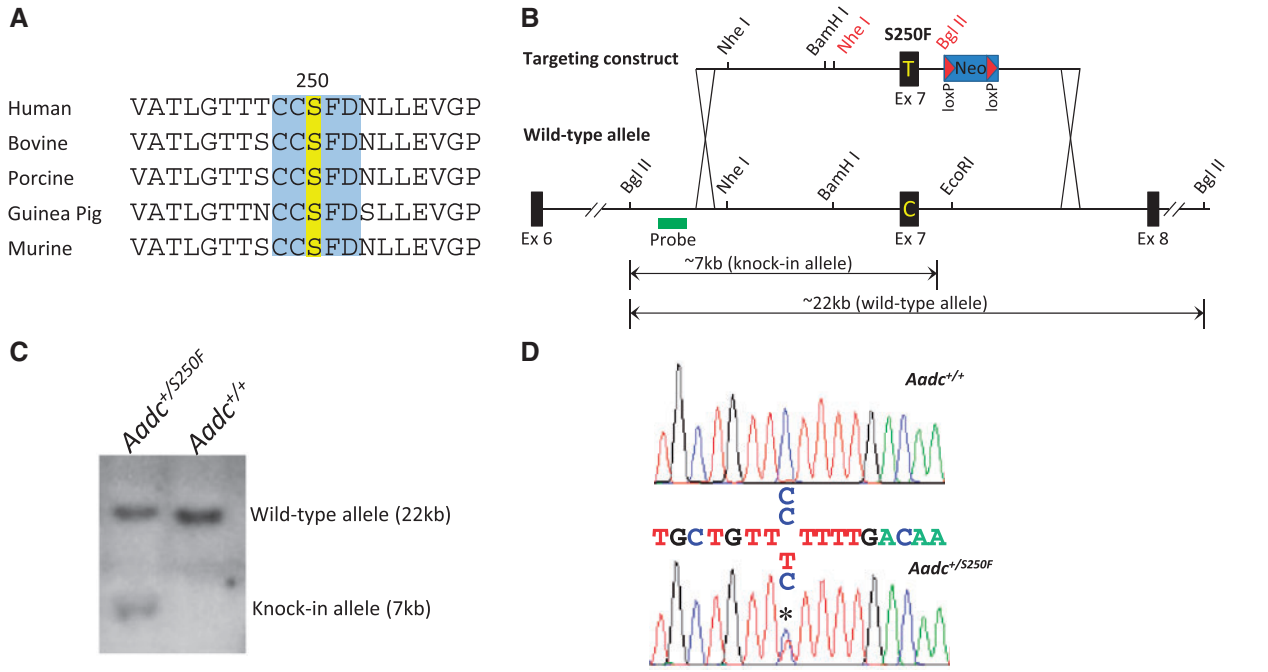

Figure 1. Generation of the S250F *Aadc* mutant mice. (**A**) A sequence alignment of the AADC proteins from various mammals. The five amino acid domain (blue) that contains the serine residue (yellow) mutated to create the $Aadc^{S250F/S250F}$ mutant mice is perfectly conserved from humans to rodents. (**B**) A schematic depicting the targeting strategy that was used to introduce the S250F mutation into the mouse genome. Indicated are the diagnostic 7 and 22 kb Bgl II fragments used to identify the mutant and wild-type *Aadc* alleles. The Nhe I and Bgl II sites in red text denote restriction sites engineered into the targeting construct. (**C**) Results of a Southern blot experiment on DNA from a correctly targeted ES cell clone and wild-type line. Whereas the probe revealed only one (22 kb) band in the wild-type cells, a second (7 kb) band corresponding to the mutant allele is also detected in the mutant ES cell clone. (**D**) Sequence chromatogram of DNA from the founder derived from the targeted ES cells reveals two peaks (asterisk) at position 890 of the mutant murine *Aadc* gene, confirming the presence of the C → T transition that gives rise to the S250F mutation. Also depicted is DNA sequence from a wild-type mouse which is homozygous C at the relevant nucleotide position.

suggest that a combination of recessively acting genetic modifiers deriving from each of the two strain backgrounds used in the study interact to suppress disease severity, overcome embryonic lethality and allow for viable mutants to be generated on a mixed strain background.

The S250F mutation disrupts AADC activity and reduces monoamine levels in mutant mice

The subjects of the initial AADC deficiency study were found to be homozygous for the S250F mutation and reported to have enzyme activity levels at ~2% of the reference mean at 9 months of age (11,16). The low activity is thought to result from a post-transcriptional effect of the S250F mutation (17); no change in mutant transcript levels were detected, but the resulting protein was found, in transiently transfected cells, to be especially prone to degradation by the ubiquitin proteasome system (17). To determine how the S250F mutation affects expression of the mutant *Aadc* allele in our model mice, we assessed transcript levels in brain tissue of the animals. As expected, we found no significant change in mutant transcript levels (Fig. 2A). We next examined mutant protein levels in brain tissue of the mice. In contrast to experiments in transfected cells, we found that *in vivo* the mutant protein is stable and expressed at equivalent levels to those of WT protein (Fig. 2B and C). To determine if the S250F mutation nevertheless affects the function of the protein, we assessed AADC activity from whole-brain tissue homogenates. We found that despite being expressed at control levels, the mutant protein exhibits minimal (<4%) activity in converting L-DOPA to dopamine (Fig. 2D). Still, we were able to detect dopamine in mutant striatum. Levels of this monoamine were reduced, but only by ~25% (Fig. 2E). Consistent with the stability of the mutant protein, immunohistochemistry studies showed that AADC was prominently expressed in the striatum of both mutant and heterozygous control mice (Supplementary Material, Fig. S2). In contrast to the somewhat limited decline in brain dopamine, serotonin levels in mid-brain tissue containing the raphe nuclei were markedly (>60%) reduced, although we were nevertheless able to detect it in brain homogenates by HPLC analysis (Fig. 2F). Mutant dorsal raphe nuclei stained just as brightly as the striatum for AADC (Supplementary Material, Fig. S2). Collectively, these results suggest that while the S250F mutation does not affect the stability of the AADC protein, it has a profound effect on enzyme function. Still, even miniscule concentrations of active enzyme are sufficient to produce considerable quantities of at least one of the two monoamines—dopamine—catalyzed by AADC.

In a fly model, absence of AADC perturbed the stereotypic patterning of catecholaminergic neurons, resulting in the appearance of a novel set of these cells in the ventral ganglion (18). On the other hand, loss of the enzyme in model mice did not reportedly affect dopaminergic neuron numbers (13). To determine how mutant AADC containing the S250F mutation might affect these cells, we examined the morphology and numbers of the neurons in the substantia nigra. We found no difference in either morphology or number of nigral neurons between mutant mice and heterozygous controls (Fig. 3A and B). Our results suggest that a major loss of AADC activity neither perturbs the patterning of the dopaminergic neurons in the substantia nigra nor results in their degeneration.

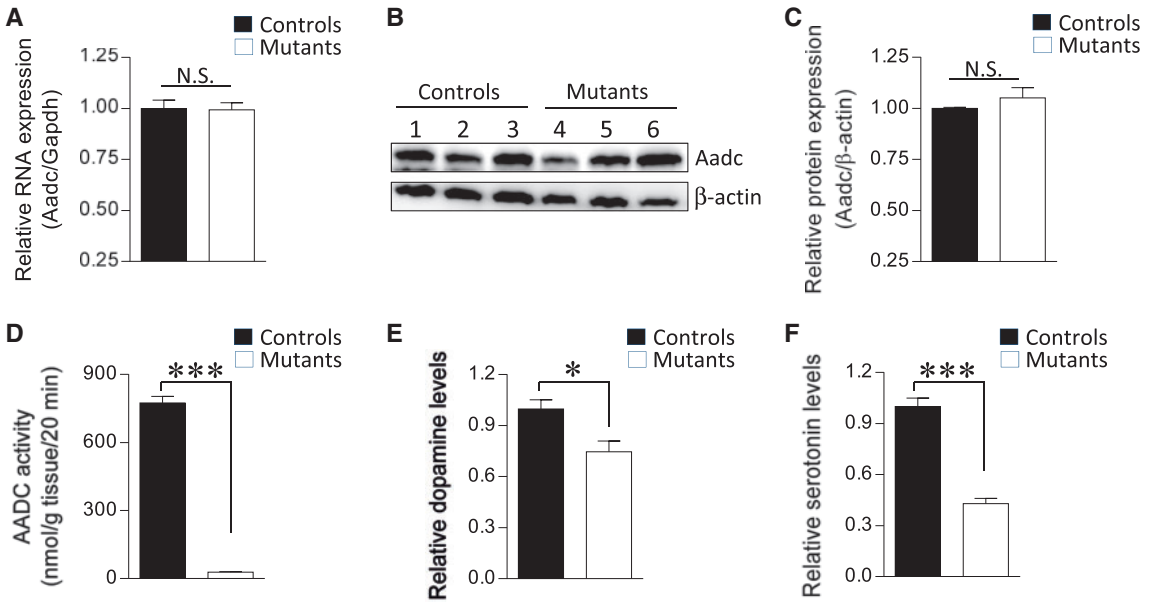

Figure 2. The S250F mutation has no effect on the expression of the mutant AADC enzyme but profoundly alters its activity. (**A**) Quantified results of real-time PCR experiments on *Aadc* transcripts expressed in brain tissue of 6-week-old mutant and littermate control ($Aadc^{+/S250F}$) mice. No difference in the expression of the mutant RNA is detected. Sample sizes of $n \geq 3$ mice of each genotype were used for the analysis. (**B**) Protein from the mutant and control mice was also found to be expressed at equivalent levels as assessed by western blot analysis. (**C**) A graph depicting the quantification of the mutant and wild-type protein detected in the blot in (B). (**D**) Notwithstanding the stable nature of the mutant AADC protein, its activity in converting L-Dopa to dopamine is severely compromised. Samples of at least five mutants and control littermates were used for the analysis. (**E**) Quantified levels of dopamine in brain striata of $Aadc^{S250F/S250F}$ mutant mice and control littermates demonstrating a ~25% reduction in the amounts of this neurotransmitter in the former cohort. (**F**) A similar quantification of serotonin levels from mid-brain homogenates of the two cohorts of mice shows a more marked depletion of this neurotransmitter in the $Aadc^{S250F/S250F}$ mutants. Sample sizes of $n \geq 6$ mice of each genotype were used to quantify brain dopamine and serotonin levels. Note: * and ***$P < 0.05$ and <0.001, respectively, *t* test.

Model mice harboring the S250F mutation exhibit behavioral and autonomic abnormalities

Severely affected AADC patients characteristically present with motor defects and autonomic dysfunction owing to reduced levels of the catecholamines and serotonin. Life expectancy is also frequently reduced. We therefore began the phenotypic assessment of our $Aadc^{S250F/S250F}$ mutants by examining survival. Given the decidedly modest drop in mutant brain dopamine in animals that survived embryonic development, we were not surprised to find that their life expectancy was not adversely affected (Supplementary Material, Fig. S3A). The mice routinely lived to 24 months or more of age. We further found that such mutants were phenotypically indistinguishable from control littermates at birth (data not shown). However, weight measurements showed that adult $Aadc^{S250F/S250F}$ mice consistently tended to be heavier than controls beginning at 6 weeks of age (Supplementary Material, Fig. S3B and Fig. 4A). In males this difference became especially prominent between 10 and 18 weeks of age (Fig. 4A). This result would be expected of mice expressing low serotonin, a neurotransmitter implicated in satiety and the suppression of feeding behavior (19,20). Magnetic resonance imaging (MRI) of AADC deficient patients is generally not remarkable. However, in a few such individuals, studies revealed evidence of cerebral atrophy (4). We therefore also measured brain volume in the $Aadc^{S250F/S250F}$ mutants. At 6 weeks of age we found that brain weights of mutant mice were no different from those of control littermates even when corrected for body weight of the animals (Fig. 4B), suggesting that in this mild model of AADC deficiency micrencephaly is not a distinct feature.

Amongst the most distinctive disease characteristics of AADC deficiency are movement defects. We therefore proceeded to examine the model mice using one particular assay, the rotarod test, commonly used to detect such defects in genetically modified rodents. We found that the mutants performed just as well as control littermates between 7 and 8 weeks of age but declined in ability thereafter; a significant difference in latency on the rotarod appeared between 11 and 12 weeks of age (Fig. 4C). Low levels of serotonin stemming from an ablation of the serotonergic neurons impact cardiovascular function and thermoregulation (15,21). Accordingly, we also examined the physiology of these functions in the mutants. We found cardiac function as measured by heart rate, cardiac output and ejection fraction to be normal in conscious model mice (Fig. 4D–F). However, we discovered that the ability of the $Aadc^{S250F/S250F}$ mice to maintain and regulate body temperature is severely compromised. Exposure to a cold (4°C) environment resulted in a decline in core body temperature of both mutants and controls (Fig. 4G). However, the drop was considerably sharper in the mutants and their body temperature lower than that of controls 30, 60 as well as 90 min following transfer of the animals to the cold. At the 30 and 60 min time points the difference between the cohorts reached statistical significance exemplified by one mutant that became so hypothermic that it had to be removed from the study. In addition to the greater hypothermia of the mutants, we also noted that they recovered less efficiently. Thus whereas control temperatures recorded at the 90 min mark were statistically equivalent to initial values, mutant temperatures remained significantly lower at this time point relative to those obtained at the start of the experiment (Fig. 4G). These results suggest at least some level of dysautonomia in the $Aadc^{S250F/S250F}$ mutants. The appearance of the motor defects in the mutants may, however, be more to do with the proclivity of these animals to become obese, owing to low serotonin, rather than defects of the

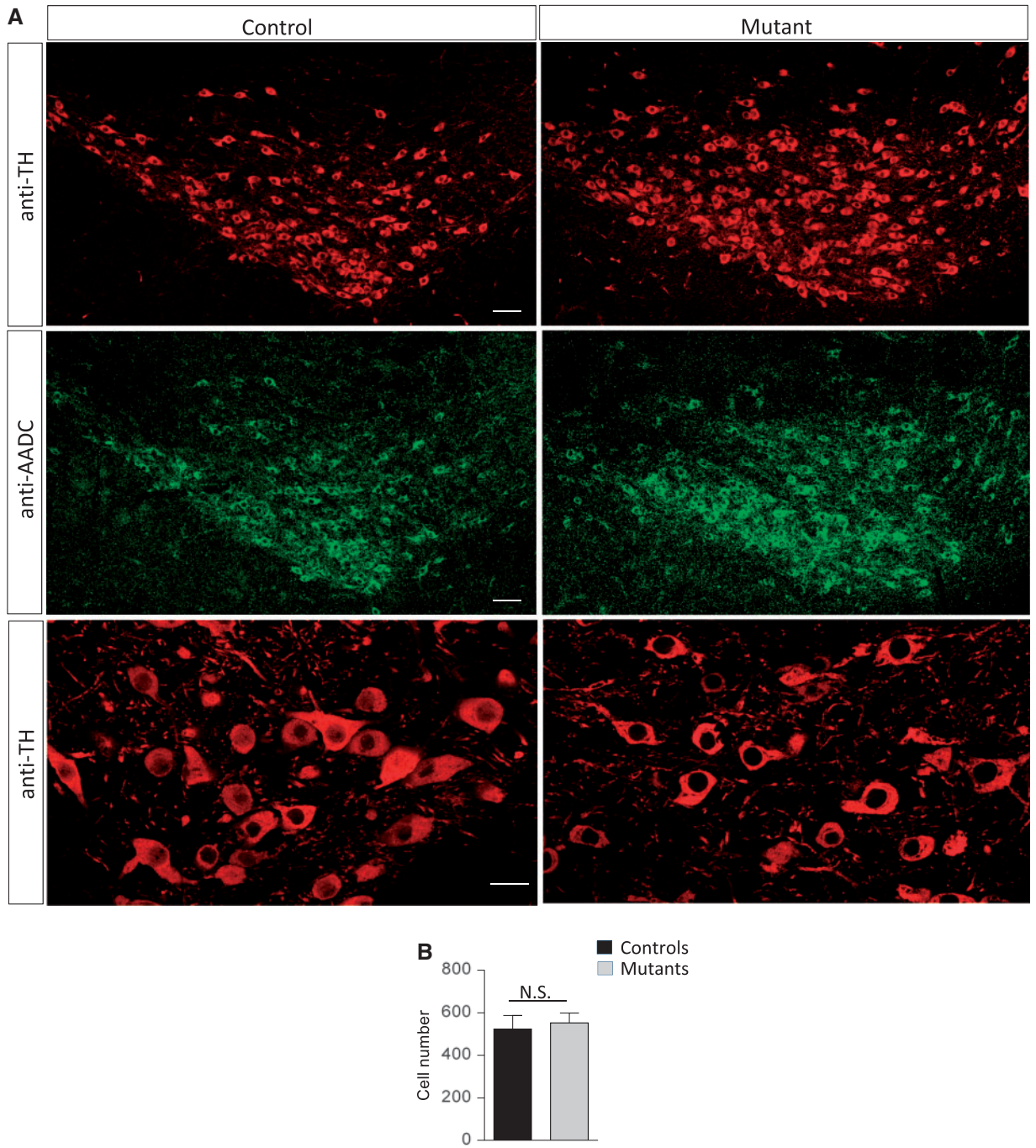

Figure 3. No evidence of neurodegeneration in *Aadc*$^{S250F/S250F}$ model mice. (**A**) Representative photomicrographs of the substantia nigra from an *Aadc*$^{S250F/S250F}$ mutant and a control littermate dual-stained with antibodies against tyrosine hydroxylase and AADC. Scale bars—100 μm, upper and middle panels, 20 μm, bottom panels. (**B**) Quantification of tyrosine hydroxylase-positive nigral neurons in brains of *Aadc*$^{S250F/S250F}$ mutants and control littermates demonstrates little evidence of cell loss in model mice. Note: N.S.—values not significant ($P > 0.05$) *t* test, $n \geq 3$ mice of each cohort.

dopaminergic system. Indeed, the motor defects became more pronounced as differences in weight between mutants and controls increased.

Discussion

AADC catalyzes the final step in the synthesis of the monoamine neurotransmitters dopamine and serotonin. Accordingly, loss-of-function mutations in the *AADC* gene result in depleted levels of the two monoamines and their downstream products. The associated condition, AADC deficiency, is a rare, severely disabling and frequently fatal pediatric onset neurodevelopmental disorder characterized by movement defects, retarded development and abnormalities of the autonomic system. There is currently no optimal treatment for AADC deficiency and few animal models bearing mutations previously identified in patients with the disease. Here, we describe a novel mouse model of mild AADC deficiency that was engineered to express a relatively common S250F

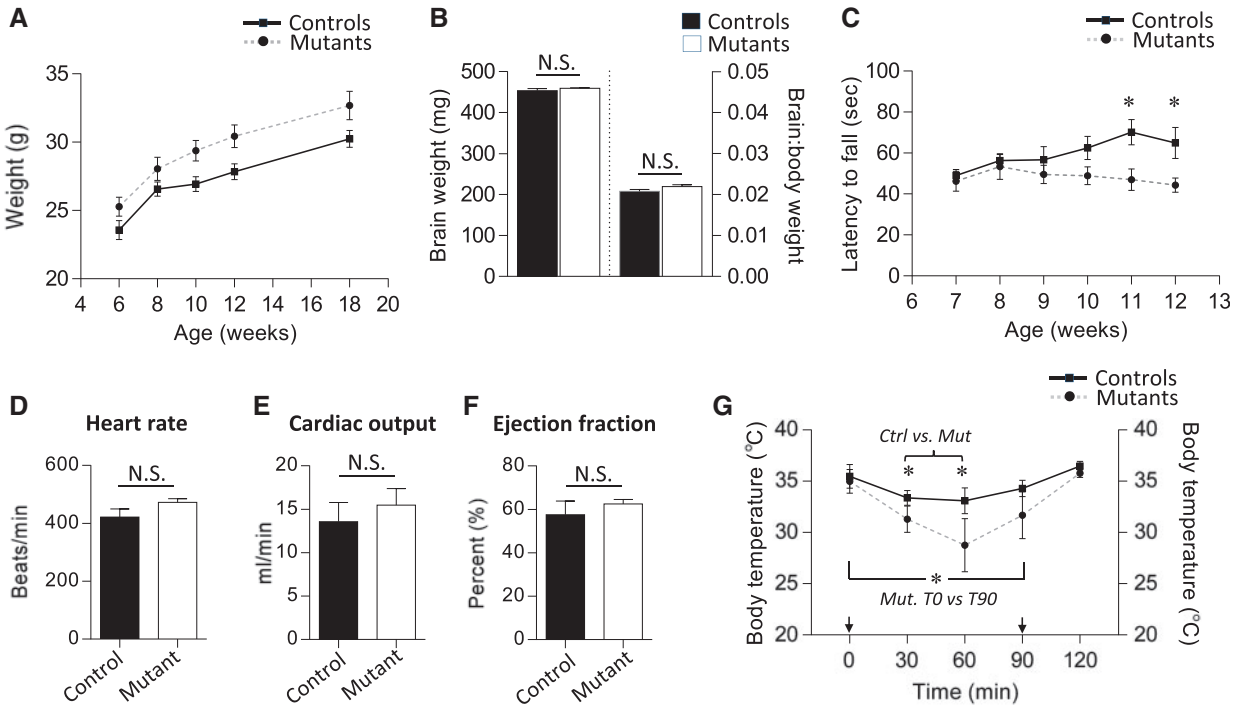

Figure 4. Evidence of behavioral defects and autonomic dysfunction in *Aadc*$^{S250F/S250F}$ mutant mice. (**A**) Weight measurements of adult male *Aadc*$^{S250F/S250F}$ mutant mice and control littermates compiled over a period of 12 weeks reveal that mutants are heavier over the entire period and markedly so from 10 weeks of age. Sample sizes of $n \geq 10$ mice of each genotype were used to generate the curves. Curves are significantly ($P = 0.0129$) different; Statmod statistical package. (**B**) Quantified results of brain weights and brain: body weight ratios in 6-week-old male *Aadc*$^{S250F/S250F}$ mutant mice and control littermates shows no difference in either parameter. $n \geq 3$. (**C**) Results of rotarod tests on *Aadc*$^{S250F/S250F}$ mutant mice ($n \geq 11$) and control littermates ($n \geq 9$) depicting the emergence of a significant difference in motor performance at 11 and 12 weeks of age. Cardiac function in *Aadc*$^{S250F/S250F}$ mutant mice was found not to be affected as determined by measuring (**D**) heart rate, (**E**) cardiac output and (**F**) ejection fraction, and comparing these parameters between mutant and control littermates. $N \geq 4$ of each cohort examined. (**G**) Low levels of active AADC enzyme have a profound effect on thermoregulation. *Aadc*$^{S250F/S250F}$ mutants experienced sharper drops in body temperature and longer recovery periods than controls when animals were subjected to a cold environment. Sample sizes of $n = 4$ mice of each genotype were used to generate the traces on the graph. The two arrows indicate when mice were initially exposed to the cold environment and then returned to room temperature respectively. Note: *$P < 0.05$, *t* test wherever applicable.

mutation identified in a cohort of such patients. Five main findings emerge from our study. First, we confirm the pathogenic nature of the S250F mutation. Model mice harboring the mutation express profoundly low levels of active protein. Yet they are viable, thus enabling not only a detailed investigation of the disease but also the pre-clinical development of relevant treatment strategies in this model system. Second, we show that despite extinguishing >95% of AADC activity in the mutant animals, dopamine levels declined by only modest amounts. Serotonin levels, on the other hand, were more markedly affected but nevertheless detectable by biochemical as well as anatomical means. We suggest that incremental increases in enzyme activity will have large effects on neurotransmitter levels and disease phenotype. We also propose that the more modest effects of the AADC S250F mutation on dopamine levels relative to serotonin concentrations may simply be a consequence of the enzyme having a much higher (>8) activity with L-Dopa than with 5-HTP as a substrate (22). Third, we demonstrate that notwithstanding the continued presence of significant levels of brain dopamine and serotonin in *Aadc*$^{S250F/S250F}$ mutants, the mice are clearly symptomatic of conditions associated with the human disease, particularly those associated with low serotonin. Defects ranging from compromised motor performance to autonomic dysfunction to poor maternal instinct were all detected in the mutants. Fourth, we conclude that neither low levels of active AADC enzyme nor reduced amounts of the monoamines and their by-products grossly affect brain structures associated with the dopaminergic or serotonergic systems. No nigral cell loss was detected—a situation that avoids the necessity of cell replacement and thus eases the design of prospective treatments for this disease vis à vis neurodegenerative conditions such as spinal muscular atrophy. Finally, our study raises the prospect of potent modifiers of the disease phenotype. We infer this from the distinct frequencies with which *Aadc*$^{S250F/S250F}$ mutants were derived on the different genetic strain backgrounds employed in the study. Identifying such modifiers will not only cast new light on basic mechanisms underlying AADC deficiency but could also be therapeutically relevant.

Our choice of the S250F mutation to generate AADC deficient model mice derived from its relatively high (~10%) frequency in the patient population and its associated mild phenotype. The resulting mild phenotype of the viable mutants was therefore not altogether surprising. Still, we were interested to discover that the S250F mutation does not lead to a decline in AADC levels. A previous study that examined the effects of this mutation concluded that it alters the tertiary structure of the protein, disrupting activity and triggering rapid degradation (17). Our *in vivo* findings are consistent with the prior report of reduced S205F AADC activity but fail to support the contention that the mutation destabilizes the enzyme. One explanation for the distinct findings is the different systems—*in vitro* versus *in vivo*—employed in arriving at our respective conclusions. However, it is also possible that lower protein levels in the cell culture study by Montioli *et al.* stemmed from reduced transfection efficiency of the mutant construct; it is unclear whether the experiment

that was undertaken in their study to control for transfection efficiency exclusively measured reverse transcribed DNA from the transfected cells or a combination of both contaminating residual DNA—from the plasmid used in the transfections—as well as its transcribed product. Still, this does not detract from the common conclusion that the S250F mutation is pathogenic irrespective of whether it is expressed in cells in culture or model mice. The $Aadc^{S250F/S250F}$ mutant mice also allow one to explore, in the mutant organism, mechanisms underlying dysfunction associated with the S250F mutation. Phenylbutyrate and pryridoxine which are reported to mitigate the mis-folding of the S250F mutant protein (17) could be tested as potential therapeutics in the mutant mice.

Considering the quite modest drop in brain levels in our $Aadc^{S250F/S250F}$ mutants, we were not surprised that a proportion of the mice was not only viable but also reached adulthood and bred. Given prior studies in dopamine as well as serotonin deficient mice (15,21,23,24), we were also not startled to find normal numbers of nigral neurons in the mutants and the appearance of a grossly intact striatum and raphe nucleus, brain structures associated, respectively, with the dopaminergic and serotonergic pathways. Nevertheless, we were reassured to find distinct and characteristic phenotypes associated with a deficit of one and/or the other neurotransmitter. Disrupted serotonin signaling has previously been reported to affect feeding behavior and satiety, cardiovascular function, maternal instincts as well as thermoregulation (15,19–21,23–25). The $Aadc^{S250F/S250F}$ mutants we generated exhibited perturbations in many of these functions. For instance, they gained disproportionately more weight than controls, failed to rear normal-sized litters owing to poor maternal care and were relatively inefficient at compensating for changes in ambient temperature, phenotypes consistent with the findings in the prior reports. It is possible that normal cardiac function in our mice arises from a continued presence of ∼40% of WT serotonin levels but could also stem from the particular point in time during the day—the morning—that the parameter was determined. $Tph2^{-/-}$ mice lacking CNS serotonin displayed reduced blood pressure and heart rate mainly in the late afternoon and night (15). In a zebrafish model of AADC deficiency, morphants' brains failed to develop normally with associated loss of dopaminergic and serotonergic neurons (26). We did not observe this, and our result is more closely aligned with those of other studies of reduced AADC (13) or the monoamines (15,23,24) in rodents. It is possible that compromised brain development in the fish model is specific to zebrafish or a consequence of very severe knockdown and undetectable AADC levels. Similar distinctions in phenotype have been noted in fish and mouse models of Glucose Transporter-1 (Glut1) deficiency syndrome, another pediatric neurodevelopmental disorder in which loss of the Glut1 protein in the fish but not the mouse triggered a breakdown of the blood-brain barrier (27,28).

Perhaps the most intriguing aspect of our study was finding how profoundly genetic strain background affects the disease phenotype in $Aadc^{-/-}$ mutants. Our findings clearly imply two quite distinct phenotypes—one characterized by embryonic lethality, the other a relatively mild phenotype that evolves during adulthood. Others have reported similar findings in distinct models. In one study, only ∼33% of $Aadc^{S250F/S250F}$ mutants were found to be viable, although genetic background was not raised as a potential explanation (13). In *Tph2* knockout mice, the disease phenotype was more severe on an FVB/N than it was on a C57Bl/6 background (15). Given disease heterogeneity in human patients and the concept of epistasis, such findings are perhaps not entirely surprising and, moreover, present exciting opportunities to exploit the observation in the mice to identify distinct modifiers as a means to better understand basic mechanisms. This could be pursued using an F1 intercross of carrier animals, deriving half of their genomes from each of the C57Bl/6 and FVB/N strains of mice, to generate mutants with the severe or mild form of the disease. In summary, we report here a novel model of AADC deficiency. To our knowledge it represents the first example of a rodent mutant that harbors an identified human AADC deficiency mutation and, moreover, exhibits a disease phenotype. We expect the mice to be useful in casting new light on basic AADC deficiency disease mechanisms and as a tool in the pre-clinical development of therapies for this devastating disorder.

Materials and Methods

Mice

BAC clone BMQ413k20 (Source Biosciences, Nottingham, UK) from a 129/SvJ library contains the murine *Aadc* gene. The clone was digested with EcoR I and a ∼9 kb fragment containing exon 7 of the gene first inserted into pUC19 and then into the pStartK (Addgene) vector. The latter was used as a template to introduce the S250F (C>T) mutation into exon 7 by means of overlapping PCR, and diagnostic Nhe I and Bgl II sites simultaneously engineered into the targeting insert. An ACN cassette consisting of the two genes *tACE-Cre/Neo*^{R} (29) flanked by loxP was then placed downstream of exon 7 using restriction enzymes. The targeting vector containing the mutant allele flanked by ∼6 and ∼3 kb left and right arms, respectively, was linearized and electroporated into ES cells. G418 resistant colonies were initially screened by PCR and then Southern blot analysis to identify correctly targeted clones. Of a total of four positive clones, one was injected into C57Bl/6 blastocysts and a single male chimera obtained. Breeding him deleted the Neo cassette leaving progeny harboring just the S250F mutation. Heterozygous animals $Aadc^{+/S250F}$ were bred with one another to generate $Aadc^{S250F/S250F}$ mutants. To transfer the mutant allele to pure strain backgrounds, carriers were backcrossed over five successive generations to each of the FVB/N and C57Bl/6 strains. In every instance, the mutant allele was distinguished from the WT allele using a multiplex PCR. Primer Seq 10F 5'-CCAATGACTGCCTTGTGGAATG-3' was used with Seq 9R 5'-GCGTGATGTCTGGCACAAGTC-3' and Seq 12R 5'-CGG TAGAATTGACCTGCAGG-3' to amplify the WT (∼420 bp) and mutant (∼350 bp) alleles. Genotyping was carried out on tail tissue using standard methods. Mice were housed under standard conditions with artificial 12 h dark–light cycles. All experiments with mice were conducted in accordance with the protocols described in the Guide for the Care and Use of Laboratory Animals (NIH. Revised 2011) and were approved by Columbia University's Institutional Laboratory Animal Care and Use Committees.

Western blotting and transcript analysis

Mice were euthanized by cervical dislocation. Brains were extracted and divided in the sagittal plane into equal halves, one for RNA analysis and the other for protein estimation. To determine levels of AADC transcripts, 2 μg of RNA was extracted using Trizol (Invitrogen Inc.), the RNA reverse transcribed using the RevertAid RT Reverse Transcription Kit (Thermofisher Inc.) according to the manufacturer's instructions and cDNA amplified and quantified on a MasterCycler RealPlex 4 (Eppendorf) real-time PCR machine. *AADC* Ex2 F 5'-GCATTGAGGGTCGTCCAGTG-3' and Ex3 R 5'-CTGGGTATGAGCTAGCCGTG-3' primers were used to amplify a

190 bp AADC fragment; GAPDH primers For 5'-CAACGGGAAGC CCATCACCA-3' and Rev 5'-CACAAACATGGGGGCATCGG-3'were used to amplify the internal control. All samples were analyzed in triplicate. Western blot experiments were performed as previously described (30) using antibodies against AADC (1:1000, Abcam, Cambridge, UK) and β-actin (1:2000, Santa Cruz Biotechnology Inc., Santa Cruz, CA, USA) The resulting bands were visualized on an ImageQuant LAS 4000 machine (GE Healthcare; NA-931) using the ECL Detection Kit (RPN 2109; GE Healthcare). Band intensities were quantified using the ImageJ software package (NIH). Heterozygous animals were used as controls. Male as well as female mice were included in the analysis.

Tests of motor and autonomic function

Rotarod tests were performed using the LE8200 rotarod (Harvard Apparatus/Panlab Inc). Adult male mice were trained for 60 s at 8 rpm three successive times and then tested on the accelerated setting to record ability to stay on the rotarod. Latency to fall was recorded. The performance of the mutants was compared with heterozygous control mice. To assess the ability of the mutant mice to regulate body temperature, the animals were transferred to a cold (4°C) environment for a period of 90 min, and then returned to room temperature. Body temperature was measured using a rectal probe (Thermalert TH-5, Physitemp Inc.) every half hour. A final reading was obtained a half hour after the mice were returned to room temperature. All of the mice analyzed were females and heterozygous animals used as controls.

Analysis of cardiovascular function

Transthoracic echocardiography was carried out under light anesthesia (1–2% isoflurane) using a Visualsonics Vevo 770 ultrasound system (Visualsonics) with a 30 MHz transducer applied to the chest wall. M-mode images and two-dimensional (2D) parasternal short-axis images at the midpapillary level were recorded. Measurements were made offline by a single observer in a group-blinded fashion. Left ventricular (LV) end-diastolic and end-systolic internal diameters were measured permitting calculation of LV fractional shortening (FS), LV end-diastolic volume, LV end-systolic volume, and ejection fraction (EF). The end-diastolic and end-systolic cavity areas were measured at the mid-papillary level by tracing the endocardial border, respectively. The LV fractional area change (%FAC) was estimated as, %FAC = [(LV end-diastolic cavity areas − LV end-systolic cavity areas)/LV end-diastolic cavity areas] × 100. Heart rates were determined by using M-mode images. All parameters represent the average of three beats. Heterozygous mice were used as controls for *Aadc*$^{S250F/S250F}$ mutants.

Morphological studies

Mice were euthanized with CO_2 gas and then perfused initially with PBS and subsequently with 4% PFA. Brains were then removed, post-fixed in 4% PFA (12 h, 4°C) and then transferred to 1X PBS (24 h, 4°C). The tissue was next embedded in 2% low-melt agarose for vibratome sections (Leica VT 1000S, Leica). A 70-μm thick coronal sections were cut on the vibratome, collected in PBS and then subjected to the following incubation steps: Blocking solution (4% normal donkey serum in PBST) for 1 h at room temperature, an overnight incubation with primary antibodies against tyrosine hydroxylase (1:500, EMD Millipore, Billerica, MA, USA) and AADC (1:500, Abcam, Cambridge, UK). After washing off excess antibody, the sections were further incubated (2 h, RT) with an Alexa Fluor 488-labeled anti-rabbit antibody to detect AADC and an Alexa Fluor 594-labeled anti-mouse antibody (Life Technologies, Grand Island, NY, USA) to detect tyrosine hydroxylase. Brain structures were imaged on a Leica SP8 confocal microscope (Leica). Tyrosine hydroxylase-positive dopaminergic cells in the substantia nigra were estimated in vibratome sections. Cells were counted in four coronal sections per sample and means calculated for each cohort of mice. Heterozygous mice served as controls for the *Aadc*$^{S250F/S250F}$ mutants. Mice of both genders were included in the analysis.

AADC activity and neurotransmitter levels

Whole brain homogenates were used to assess AADC activity. The assay was based on measurements of dopamine synthesized from L-DOPA and detected electrochemically using a Coulochem-II detector (ESA Inc.). The reaction mixture consisted of 30 mM sodium phosphate buffer (pH 7.2), 0.17 mM ascorbic acid, 0.1 mM pargyline HCl (an MAO inhibitor), 0.01 mM pyridoxal phosphate and 0.01 mM L-DOPA in a total volume of 400 μl. The reaction was allowed to occur at 37°C for 20 min [also see (13)]. To measure dopamine and serotonin levels, striatal and midbrain sections, respectively, were immediately dissected from euthanized 6-week-old mice, deproteinized with 0.5 M perchloric acid and centrifuged at 10, 000 rpm for 10 min. Monoamine levels were determined by HPLC with electrochemical detection as previously described (31,32). Molar amounts of metabolites were calculated from areas under HPLC peaks using calibration curves and normalized to protein concentrations in each sample.

Statistics

Kaplan–Meier survival curves were compared and assessed for differences using the log-rank test equivalent to the Mantel–Haenszel test. The unpaired, two-tailed Student's *t* test or 1-way ANOVA followed by Tukey's post hoc comparison, where indicated, were used to compare means for statistical differences. Weight curves which were constructed based on longitudinal data were analyzed using the Statmod statistical package (33). Observed and expected frequencies of mutant and control mice generated from the breeding experiments were compared for differences using the χ^2 test (GraphPad QuickCalcs). Data are represented as mean ± SEM unless otherwise indicated. $P < 0.05$ was considered significant. Statistical analyses were performed with GraphPad Prism v6.0 (GraphPad Software).

Supplementary Material

Supplementary Material is available at *HMG* online.

Acknowledgements

We thank Darryl De Vivo for comments and advice, Barbara Han for assistance with deriving the S250F embryonic stem cells and Monica Mendelsohn for generating the *Aadc* mutant mice. We are also grateful to Karen Duff, Robert Whittington and David Sulzer for access to essential equipment that made our analyses possible.

Conflict of Interest statement. None declared.

Funding

This work was supported by grants from the Pediatric Neurotransmitter Disease (PND) Association, the AADC Research Trust and the National Institutes of Health (NS057482 to U.R.M. and NS075222 to E.V.M.).

References

1. Lovenberg, W., Weissbach, H. and Udenfriend, S. (1962) Aromatic L-amino acid decarboxylase. *J. Biol. Chem.*, **237**, 89–93.
2. Berry, M.D., Juorio, A.V., Li, X.M. and Boulton, A.A. (1996) Aromatic L-amino acid decarboxylase: a neglected and misunderstood enzyme. *Neurochem. Res.*, **21**, 1075–1087.
3. Pons, R., Ford, B., Chiriboga, C.A., Clayton, P.T., Hinton, V., Hyland, K., Sharma, R. and De Vivo, D.C. (2004) Aromatic L-amino acid decarboxylase deficiency: clinical features, treatment, and prognosis. *Neurology*, **62**, 1058–1065.
4. Brun, L., Ngu, L.H., Keng, W.T., Ch'ng, G.S., Choy, Y.S., Hwu, W.L., Lee, W.T., Willemsen, M.A.A.P., Verbeek, M.M. and Wassenberg, T. (2010) Clinical and biochemical features of aromatic L-amino acid decarboxylase deficiency. *Neurology*, **75**, 64–71.
5. Lee, H.F., Tsai, C.R., Chi, C.S., Chang, T.M. and Lee, H.J. (2007) Aromatic L-amino acid decarboxylase deficiency in Taiwan. *Eur. J. Paediatr. Neurol.*, **13**, 135–140.
6. Swoboda, K.J., Hyland, K., Goldstein, D.S., Kuban, K.C., Arnold, L.A., Holmes, C.S. and Levy, H.L. (1999) Clinical and therapeutic observations in aromatic L-amino acid decarboxylase deficiency. *Neurology*, **53**, 1205–1211.
7. Wassenberg, T., Molero-Luis, M., Jeltsch, K., Hoffmann, G.F., Assmann, B., Blau, N., Garcia-Cazorla, A., Artuch, R., Pons, R., Pearson, T.S. *et al.* (2017) Consensus guideline for the diagnosis and treatment of aromatic L-amino acid decarboxylase (AADC) deficiency. *Orphanet. J. Rare Dis.*, **12**, 12.
8. Allen, G.F., Land, J.M. and Heales, S.J. (2009) A new perspective on the treatment of aromatic L-amino acid decarboxylase deficiency. *Mol. Genet. Metab.*, **97**, 6–14.
9. Manegold, C., Hoffmann, G.F., Degen, I., Ikonomidou, H., Knust, A., Laaß, M.W., Pritsch, M., Wilichowski, E. and Hörster, F. (2009) Aromatic L-amino acid decarboxylase deficiency: clinical features, drug therapy and follow-up. *J. Inherit. Metab. Dis.*, **32**, 371–378.
10. Hwu, W.L., Muramatsu, S., Tseng, S.H., Tzen, K.Y., Lee, N.C., Chien, Y.H., Snyder, R.O., Byrne, B.J., Tai, C.H. and Wu, R.M. (2012) Gene therapy for aromatic L-amino acid decarboxylase deficiency. *Sci. Transl. Med.*, **4**, 134ra61.
11. Hyland, K. and Clayton, P.T. (1990) Aromatic amino acid decarboxylase deficiency in twins. *J. Inherit. Metab. Dis.*, **13**, 301–304.
12. Montioli, R., Dindo, M., Giorgetti, A., Piccoli, S., Cellini, B. and Voltattorni, C.B. (2014) A comprehensive picture of the mutations associated with aromatic amino acid decarboxylase deficiency: from molecular mechanisms to therapy implications. *Hum. Mol. Genet.*, **23**, 5429–5440.
13. Lee, N.-C., Shieh, Y.-D., Chien, Y.-H., Tzen, K.-Y., Yu, I.-S., Chen, P.-W., Hu, M.-H., Hu, M-k., Muramatsu, S-i., Ichinose, H. and Hwu, W.-L. (2013) Regulation of the dopaminergic system in a murine model of aromatic L-amino acid decarboxylase deficiency. *Neurobiol. Dis.*, **52**, 177–190.
14. Zhang, M.Z., Yao, B., Wang, S., Fan, X., Wu, G., Yang, H., Yin, H., Yang, S. and Harris, R.C. (2011) Intrarenal dopamine deficiency leads to hypertension and decreased longevity in mice. *J. Clin. Invest.*, **121**, 2845–2854.
15. Alenina, N., Kikic, D., Todiras, M., Mosienko, V., Qadri, F., Plehm, R., Boye, P., Vilianovitch, L., Sohr, R., Tenner, K., Hortnagl, H. and Bader, M. (2009) Growth retardation and altered autonomic control in mice lacking brain serotonin. *Proc. Natl. Acad. Sci. U.S.A.*, **106**, 10332–10337.
16. Hyland, K. and Clayton, P.T. (1992) Aromatic L-amino acid decarboxylase deficiency: diagnostic methodology. *Clin. Chem.*, **38**, 2405–2410.
17. Montioli, R., Oppici, E., Cellini, B., Roncador, A., Dindo, M. and Voltattorni, C.B. (2013) S250F variant associated with aromatic amino acid decarboxylase deficiency: molecular defects and intracellular rescue by pyridoxine. *Hum. Mol. Genet.*, **22**, 1615–1624.
18. Budnik, V., Martin-Morris, L. and White, K. (1986) Perturbed pattern of catecholamine-containing neurons in mutant Drosophila deficient in the enzyme dopa decarboxylase. *J. Neurosci*, **6**, 3682–3691.
19. Simansky, K.J. (1996) Serotonergic control of the organization of feeding and satiety. *Behav. Brain Res.*, **73**, 37–42.
20. Watanabe, H., Nakano, T., Saito, R., Akasaka, D., Saito, K., Ogasawara, H., Minashima, T., Miyazawa, K., Kanaya, T., Takakura, I. *et al.* (2016) Serotonin improves high fat diet induced obesity in mice. *PLoS One*, **11**, e0147143.
21. Hodges, M.R., Tattersall, G.J., Harris, M.B., McEvoy, S.D., Richerson, D.N., Deneris, E.S., Johnson, R.L., Chen, Z.F. and Richerson, G.B. (2008) Defects in breathing and thermoregulation in mice with near-complete absence of central serotonin neurons. *J. Neurosci.*, **28**, 2495–2505.
22. Verbeek, M.M., Geurtz, P.B.H., Willemsen, M.A.A.P. and Wevers, R.A. (2007) Aromatic-L-amino acid decarboxylase enzyme activity in deficient patients and heterozygotes. *Mol. Genet. Metab.*, **90**, 363–369.
23. Zhou, Q.Y. and Palmiter, R.D. (1995) Dopamine-deficient mice are severely hypoactive, adipsic, and aphagic. *Cell*, **83**, 1197–1209.
24. Gutknecht, L., Waider, J., Kraft, S., Kriegebaum, C., Holtmann, B., Reif, A., Schmitt, A. and Lesch, K.P. (2008) Deficiency of brain 5-HT synthesis but serotonergic neuron formation in Tph2 knockout mice. *J. Neural. Transm. (Vienna)*, **115**, 1127–1132.
25. Leibowitz, S.F. and Alexander, J.T. (1998) Hypothalamic serotonin in control of eating behavior, meal size, and body weight. *Biol. Psychiatry*, **44**, 851–864.
26. Shih, D.F., Hsiao, C.D., Min, M.Y., Lai, W.S., Yang, C.W., Lee, W.T. and Lee, S.J. (2013) Aromatic L-amino acid decarboxylase (AADC) is crucial for brain development and motor functions. *PLoS One*, **8**, e71741.
27. Zheng, P.P., Romme, E., van der Spek, P.J., Dirven, C.M., Willemsen, R. and Kros, J.M. (2010) Glut1/SLC2A1 is crucial for the development of the blood–brain barrier in vivo. *Ann. Neurol.*, **68**, 835–844.
28. Tang, M., Gao, G., Rueda, C.B., Yu, H., Thibodeaux, D.N., Awano, T., Engelstad, K.M., Sanchez-Quintero, M.-J., Yang, H., Li, F. *et al.* (2017) Brain microvasculature defects and Glut1 deficiency syndrome averted by early repletion of the glucose transporter-1 protein. *Nat. Commun.*, **8**, 14152.
29. Bunting, M., Bernstein, K.E., Greer, J.M., Capecchi, M.R. and Thomas, K.R. (1999) Targeting genes for self-excision in the germ line. *Genes Dev.*, **13**, 1524–1528.
30. Kariya, S., Park, G.H., Maeno-Hikichi, Y., Leykekhman, O., Lutz, C., Arkovitz, M.S., Landmesser, L.T. and Monani, U.R. (2008) Reduced SMN protein impairs maturation of the neuromuscular junctions in mouse models of spinal muscular atrophy. *Hum. Mol. Genet.*, **17**, 2552–2569.

31. Larsen, K.E., Schmitz, Y., Troyer, M.D., Mosharov, E., Dietrich, P., Quazi, A.Z., Savalle, M., Nemani, V., Chaudhry, F.A., Edwards, R.H. *et al.* (2006) Alpha-synuclein overexpression in PC12 and chromaffin cells impairs catecholamine release by interfering with a late step in exocytosis. *J. Neurosci.*, **26**, 11915–11922.
32. Feigin, A., Fukuda, M., Dhawan, V., Przedborski, S., Jackson-Lewis, V., Mentis, M.J., Moeller, J.R. and Eidelberg, D. (2001) Metabolic correlates of levodopa response in Parkinson's disease. *Neurology*, **57**, 2083–2088.
33. Elso, C.M., Roberts, L.J., Smyth, G.K., Thomson, R.J., Baldwin, T.M., Foote, S.J. and Handman, E. (2004) Leishmaniasis host response loci (lmr13) modify disease severity through a Th1/Th2-independent pathway. *Genes Immunity*, **5**, 93–100.